Journal of Applied Electrochemistry (2006) 36:1231–1235
DOI 10.1007/s10800-006-9176-1


# Stochastic simulations of electrochemical electron transfer reactions

J. GRIMMINGER* and W. SCHMICKLER
*Department of Theoretical Chemistry, University of Ulm, D-89069, Ulm, Germany*
*(*author for correspondence, e-mail: jens.grimminger@uni-ulm.de)*

Received 30 August 2005; accepted in revised form 27 February 2006

*Key words:* electron transfer reactions, stochastic simulation

**Abstract**

The rate of electron transfer reaction has been investigated by stochastic molecular dynamics. The electronic transition probability was calculated from the Landau–Zener formula, and the coupling strength was varied over a wide region, covering both the adiabatic and the non-adiabatic regime. For low coupling, the results of first order perturbation theory are recovered, for high coupling Kramers theory is valid, and the simulations bridge these two regions.

## 1. Introduction

In the early theories of electron transfer reactions in condensed media, as developed by Marcus [1] and Hush [2], it was assumed that the reaction proceeds adiabatically, i.e. that the interaction between the reactants is so strong that an electron transfer takes place whenever the system crosses the saddle point. As was later pointed out by Zusman [3], the pre-exponential factor is then determined by solvent dynamics. In contrast, the first quantum-mechanical theories of electron transfer proposed by Levich and Dogonadze [4, 5] were based on first-order perturbation theory, and thus assumed a weak interaction and a nonadiabatic regime, in which electron transfer is rare.

There have been several attempts to bridge the gap between the adiabatic and nonadiabatic classes of theories. For the case of homogeneous reactions various approximate schemes have been proposed (see e.g. [6, 7] and references therein). For electrochemical reactions Mohr and Schmickler [8] have derived an exact expression for the transition rate, which is valid for all interaction strengths, as long as solvent dynamics is not rate determining. The same authors later combined their formalism electron transfer with solvent dynamics in order to determine the transition between the nonadiabatic and the adiabatic regimes [9].

It had already been pointed out by Levich and Dogonadze [4, 5] that the probability of an electron transfer could be calculated from the Landau–Zener formula [10, 11]. However, it is not obvious how to combine this formula with solvent dynamics. For the case of overdamped solvent dynamics this was recently achieved by one of us [12] by solving the diffusion equation with appropriate boundary conditions. In this work, we want to combine the Landau–Zener formula with stochastic simulations in order to obtain results that are valid for all values of the friction coefficient of the solvent.

## 2. Model for an electron-transfer reaction

We consider an outer-sphere electron-transfer reaction between two reactants in solution or one reactant in solution and a metal electrode. Since we are mainly interested in the effects of the electronic interaction and the solvent friction, we assume that the system is at equilibrium and do not vary the reaction free energy. The reaction is coupled to solvent modes, which are classical. Therefore they can be represented by a single effective coordinate $q$, which is equal to the reaction coordinate in the theory of Hush [2]. Using the harmonic approximation, the diabatic potential energy curves for the oxidized and the reduced state can be represented by parabolas; they can be normalized such that the equilibrium positions for the initial and final states are at $q_i = 0$ and $q_f = 1$, respectively, and the intersection point at $q_s = 0.5$, which is also the saddle point of the reaction (see Figure 1). As is common in theories of electron transfer, the frequencies $\omega$ are taken as equal in the initial and the final well. Our approach applies also to homogeneous electron transfer in solutions; in electrochemical systems, the use of single potential energy curves implies the extended Anderson–Newns model [13].

The redox system is coupled to a heat bath, which induces random motion along these potential energy surfaces. Initially, the system is placed at the minimum of the left well at $q = q_i = 0$. By thermal excitation it

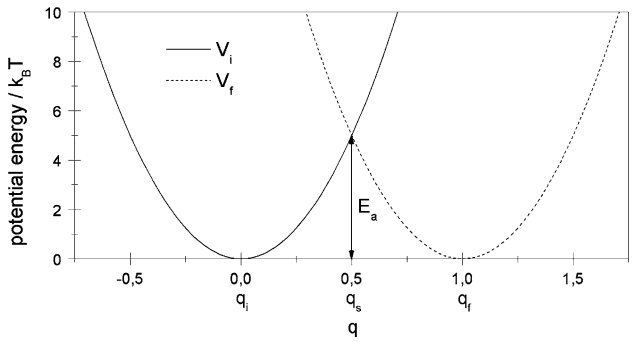


*Fig. 1.* Potential energy curves for the simulation of an electron transfer reaction at equilibrium; $V_i$: initial state, $V_f$: final state, $E_a$: activation energy.

can reach the saddle point; depending on the strength of the electronic interaction, an electron transfer may then occur. If it does, the system relaxes towards the new equilibrium position at $q = q_f = 1$; otherwise it returns to the initial well.

## 3. Simulation method

The stochastic motion of the system, caused by the coupling to the heat bath, is modelled by Langevin dynamics. According to this theory, the influence of the heat bath is expressed by a friction force $F_f$, which is proportional to the velocity of the system, and a random force $F_r$. These two parts are combined in the Langevin-equation, a model differential equation for Brownian dynamics:

$$m\frac{d^2q}{dt^2} = F_f + F_r + F_s = -m\gamma\frac{dq}{dt} + mL(t) - \frac{dV(q)}{dq} \quad (1)$$

$F_s$ is the system force due to the potential energy $V(q)$, and $\gamma$ denotes the friction coefficient, which has the dimension of an inverse time. The random term $L(t)$ must obey the following constraints: (1) The average effect of the random force must be the same in positive and in the negative q-direction:

$$\langle L(t)\rangle = 0 \quad (2)$$

(2) The random forces at different times are not correlated.

$$\langle L(t)L(t')\rangle = \Gamma\delta(t-t') \quad (3)$$

(3) The fluctuation-dissipation theorem connects the constant $\Gamma$ with the friction coefficient [14]:

$$\Gamma = \gamma\frac{2k_BT}{m} \quad (4)$$

This implies that the fluctuations are proportional to the damping at a given temperature $T$. For the implementation of the Langevin dynamics in a Verlet-like algorithm see [15, 16, 17].

For the simulations the following parameters were used: The effective mass of the harmonic oscillator was set to unity. For the energy of activation an intermediate value of $5k_BT$ was taken. This value is sufficiently low, so that even for small electronic transition probabilities a reasonable number of reactions occur within the computing time available; on the other hand it is so high that a system starting at rest gets thermalized before a transition occurs. With these values, the period of an undisturbed harmonic oscillator follows as $2\pi/\omega = 2\pi/\sqrt{40} \approx 0.99$; the time step for the simulations was set to $\delta t = 0.01$. Our simulations start with the system in the oxidized state at $q_i = 0$. During the subsequent simulation, every time the system passes the saddle point $q_s$ it is checked if an electron transfer does occur or not. For the electronic transition probability the Landau–Zener expression [10–12] is used:

$$t(\mathrm{v}) = 1 - \exp(-2\pi v) \quad \text{with } v = \frac{|\mathrm{V}|^2}{\hbar\mathrm{m}\omega^2|\mathrm{q_f v}|} \quad (5)$$

$V$ is the matrix element for the electronic coupling, and v is the velocity of the system at the saddlepoint $q_s$. Since in our model the saddle point is cusped-shaped, the velocity does not change in this critical region.

A reaction is regarded as successful when the system is in the final state and reaches a value of $q = q_b = 0.7$. The exact value of this arbitrarily chosen boundary plays no role because the system moves fast due to the steepness of the potential energy curve in this region. However, $q_b$ must be far enough from the saddle point to avoid recrossings that could bring the system back to the initial state. After a successful electron transfer the reaction time $\Delta t$ is recorded and the system starts again at $q_i$. The reaction rate $k$ is the inverse of the average reaction time $\Delta t$:

$$k = \frac{1}{\langle\Delta t\rangle} \quad (6)$$

In all simulations we averaged over at least 1000 reactions for each $k$.

## 4. Results and discussion

### 4.1. *Dependence of the reaction rate on the strength of the electronic interaction*

Figure 2 shows the dependence of the reaction rate $k$ on the Landau–Zener parameter $\sigma = |V|^2/\hbar m\omega^2 q_f$ for different values of the friction coefficient $\gamma$. For small electronic coupling the rate is proportional to $\sigma$, and thus proportional to $|V|^2$, in accordance with the predictions of the quantum theory based on first-order perturbation originated by Levich [4] and Dogonadze [5]. For high interactions $k$ attains a constant value $k_{\mathrm{limit}}$ because solvent dynamics now becomes the rate-determining factor. In the region of low friction this limiting

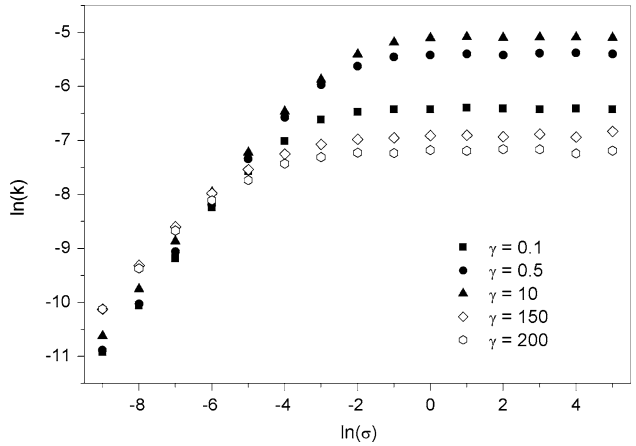


*Fig. 2.* Reaction rate versus the Landau–Zener parameter σ.

rate increases with increasing γ, whereas for higher friction $k_{\text{limit}}$ decreases with increasing γ, so there is a friction value in-between with a maximum limiting rate. In the next section this effect is investigated further.

For high friction our results are in good agreement with the calculations for the overdamped limit [12], and they also agree qualitatively with the simulations of Schmickler and Mohr [9] for nonadiabatic electron transfer reactions. A quantitative comparison with the latter work is not possible because of the different formalism employed for the transition probability. For the strongly adiabatic case one should expect again a rise of the reaction rate [9] because the energy of activation is lowered. This effect was not observed in our simulations since we use diabatic potential energy curves whose shapes are independent of the strength of the electronic coupling.

### 4.2. *Dependence of the reaction rate on the friction in the adiabatic limit*

In Figure 3 a plot of the limiting rate versus the friction coefficient is shown. In these simulations the Landau–Zener parameter σ is set to $e^5$ so the transition probability was practically unity. This plot shows the behaviour predicted by Kramers theory: The rate increases rapidly in the low friction region, reaches a maximum at $\gamma \approx 3.5$ – this is the Kramers turnover region –, and decreases slowly for higher γ. At very low friction values the interaction between the heat bath and the redox system is so weak that the system rarely gets enough energy to reach the saddle point. As a consequence, the rate increases with increasing γ. However, the higher the friction, the higher the number of recrossings of the saddle point, and the higher the viscosity. Both effects eventually lead to a decrease of the rate constant. Figure 4 illustrates these effects: it shows a plot of the number of electron transfer reactions, the crossings of the saddle point and the recrossings versus the friction coefficient.

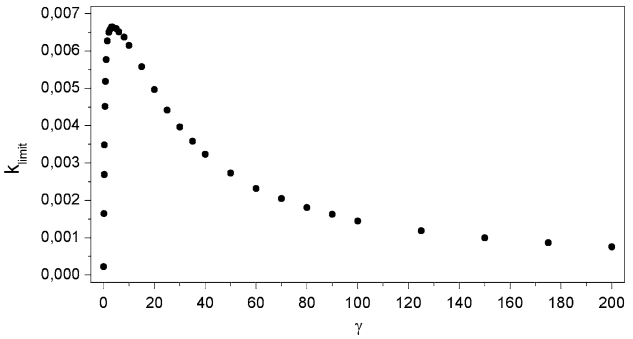


*Fig. 3.* Reaction rate versus the friction coefficient γ in the adiabatic limit.

The recrossings are calculated as follows:

$$\text{recrossings} = \frac{\text{crossings of saddle point} - \text{number of reactions}}{2}$$

The curve of the reaction number has the same shape as those in Figure 3 since the reaction rate can also be calculated as the ratio of the reaction number and the simulation time τ, which has been constant for all γ-values ($\tau = 10^7$). The steep rise of this curve in the region of very low friction is only due to the steep increase of the saddle point crossings since the number of recrossings is very low and first begins to increase markedly at $\gamma \approx 5$. After reaching the maximum at $\gamma \approx 3.5$, the number of reactions falls strongly because there is a sharp rise of the recrossings curve. The latter attains from $\gamma \approx 80$ on a rather constant value and the reaction curve flattens out since only the slowly decreasing saddle point crossings due to the ascending viscosity gives rise now to the decrease of the reaction number.

These results agree quantitatively and qualitatively with Kramers' turnover theory [18], which predicts a proportionality between the reaction rate and the friction coefficient in the low friction region, and an inverse proportionality in the high friction region:

$$k = \frac{1}{2}\gamma \frac{E_a}{k_B T} \exp\left(-\frac{E_a}{k_B T}\right) \quad \text{low friction} \tag{8}$$

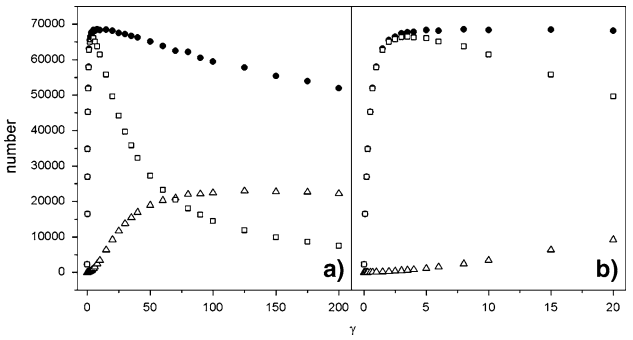


*Fig. 4.* (a) Number of saddle point crossings (●), electron transfer reactions (□) and recrossings (△) in dependence of the friction coefficient during $10^7$ time units; (b) Region of low friction.

$$k = \frac{\omega^2}{2\pi\gamma}\sqrt{\pi\frac{E_a}{k_B T}}\exp\left(-\frac{E_a}{k_B T}\right) \text{ high friction} \qquad (9)$$

Figure 5 shows the comparison of our results with Kramers' theory. Since equations (8) and (9) give limiting values for very low/high friction, the agreement with the rate constants of the simulations becomes better with lower/higher γ.

A similar dependence of the rate constant on the friction coefficient was obtained in earlier simulations of an adiabatic bond breaking electron transfer reaction on a metal electrode [19].

### 4.3. *Dependence of the normalized reaction rate on friction*

An interesting problem is the effect of the friction on the electronic transition probability in the non-adiabatic regime. In order to illustrate this effect we have investigated the dependence of the normalized reaction rate $k_{\mathrm{no}} = \frac{k}{k_{\mathrm{limit}}}$ on the friction. Figure 6 shows two plots of $k_{\mathrm{no}}$ versus γ, where $k$ is the rate constant with the Landau–Zener parameter $\sigma = e^{-2}$ and $\sigma = e^{-4}$ respectively. $k_{\mathrm{limit}}$ is the reaction rate in the adiabatic limit with $\sigma = e^{5}$.

Both curves have the same form: In the region of very low friction they decrease strongly, then go through a minimum at $\gamma \approx 3.5$ – the same value as the maximum in Figure 3 – and increase slowly with higher friction. At the minimum $k_{\mathrm{no}}$ equals an effective transition probability $t_{\mathrm{eff}} = \frac{2t(v)}{1+t(v)}$, which accounts for multiple crossing of the saddle point [20] (see table 1). $t$(v) is obtained from the simulations: $t$(v) = transitions/crossings of the saddle point. At $\gamma \approx 3.5$ the friction is optimal; there are very few recrossings and the decelerating effect of the viscosity is also still negligible. So the only rate-determining factor is the transition probability, whose value is reflected in $k_{\mathrm{no}}$.

For very low friction $k_{\mathrm{no}}$ approaches unity because in the non-adiabatic case the system has more attempts for a transition since, once it has reached the saddle point, it keeps the high energy for a certain time. After each oscillation it crosses the saddle point again because the low friction entails a low damping.

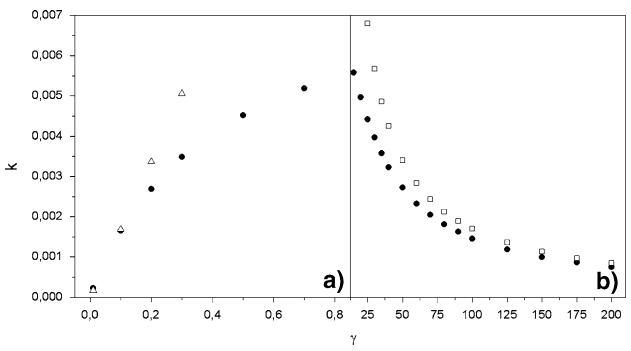


*Fig. 5.* Comparison of the simulation results (●) with Kramers' theory ( △, □) in the region of low (a) and high (b) friction.

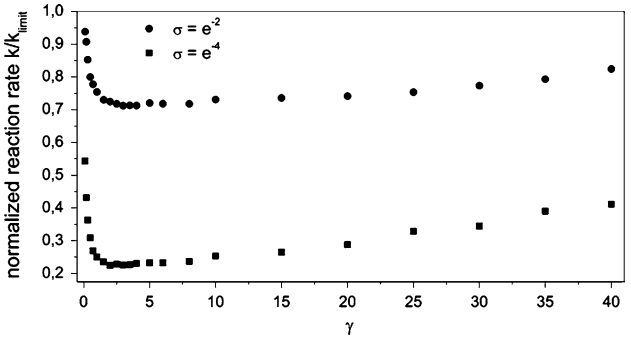


*Fig. 6.* Dependence of the normalized rate $k/k_{\mathrm{limit}}$ on the friction coefficient γ.

The slow increase of $k_{\mathrm{no}}$ for $\gamma > 3.5$ has three reasons: First, the higher the friction the slower the movement of the system. This leads to a higher transition probability $t$(v) (cf. equation (5) and Table 1). Second, at higher friction the system performs more recrossings. In the nonadiabatic case the probability of changing to the potential curve of the initial state during a recrossing is lower, so the system may just be reflected at the saddle point. In the adiabatic case however the system always ends up in the initial state after a recrossing. Third, the higher the transition probability and the friction, the greater the deviation from Boltzmann equilibrium. The system's duration of stay at higher energies (saddle point region) is shorter than predicted by the Boltzmann equilibrium because, after the transition to the final state and the passing of $q_b$, the reaction is complete, and the system starts again in the initial well. The higher the friction, the longer it takes to reach the saddle point again, and the higher is the discrepancy between the durations of stay at high and low energies. For low transition probabilities the system remains a longer time in the saddle point region once it has gained the necessary energy and thus has multiple attempts for a successful transition. The first effect does not depend on the Landau–Zener parameter σ, whereas the last two effects become more important with decreasing transition probability. Hence the curve for $\sigma = e^{-4}$ shows a steeper slope than that of the more adiabatic case with $\sigma = e^{-2}$.

## 5. Conclusions

Using the Landau–Zener formula for the electronic transition probability, we have investigated the dependence of the electron transfer rate on the strength of the

*Table 1.* Transition probabilities and $k/k_{\mathrm{limit}}$ obtained from the simulations at two different friction coefficients and coupling strengths

| σ | γ | $t$(v) | $t_{\mathrm{eff}}$ | $k_{\mathrm{no}}$ |
|---|---|---|---|---|
| $e^{-2}$ | 3.5 | 0.54 | 0.70 | 0.71 |
| $e^{-4}$ | 3.5 | 0.13 | 0.23 | 0.23 |
| $e^{-2}$ | 40.0 | 0.60 | 0.75 | 0.82 |
| $e^{-4}$ | 40.0 | 0.17 | 0.29 | 0.41 |

electronic coupling by stochastic molecular dynamics simulations. Our results cover the whole range from the non-adiabatic to the adiabatic regime, and thus encompass the validity range of both first-order perturbation and of Kramers theory. In addition, our work covers the whole friction range from the underdamped to the overdamped region, and holds both for electrochemical and for homogeneous electron transfer. On the whole, it is in line with previous results, but it covers a wider range and adds important details. In particular, the subtle interplay between the friction and the electronic transition probability discussed in the last paragraph sheds new light on the nature of non-adiabatic electron transfer.

## Acknowledgments

Financial support by the Deutsche Forschungsgemeinschaft is gratefully acknowledged. J.G. would like to thank the Fonds der Chemischen Industrie for a fellowship.

## References

1. R.A. Marcus, *J. Chem. Phys.* **24** (1956) 966.
2. N.S. Hush, *J. Chem. Phys.* **28** (1958) 962.
3. L.D. Zusman, *Chem. Phys.* **49** (1980) 295.
4. V.G. Levich. *in* H. Eyring, D. Henderson and W. Jost (Eds), Kinetics of Reactions with charge Transfer in: Physical Chemistry, an Advanced Treatise, Vol. Xb, (Academic Press, New York, 1970).
5. R.R. Dogonadze. *in* N.S. Hush (Ed), Reactions of Electrons at Electrodes, (Interscience, London, 1971).
6. A.A. Stuchebrikhov and X. Song, *J. Chem. Phys.* **101** (1994) 9354.
7. C.D. Schwieters and G.A. Voth, *J. Chem. Phys.* **108** (1998) 1005.
8. J. Mohr and W. Schmickler, *Phys. Rev. Lett.* **84** (2000) 1051.
9. W. Schmickler and J. Mohr, *J. Chem. Phys.* **117** (2002) 2867.
10. L.D. Landau and E.M. Lifshitz, *Quantum Mechanics* (Pergamon, Oxford, 1965).
11. C. Zener, *Proc. Roy. Soc.* **137** (1932) 696.
12. W. Schmickler, *Condensed Matter Physics* **4** (2001) 773.
13. W. Schmickler, *J. Electroanal. Chem.* **204** (1986) 31.
14. N.G. van Kampen, *Stochastic Processes in Physic and Chemistry* (North Holland, Amsterdam, 1981).
15. M.P. Allen and D.J. Tildesley, *Computer Simulation of Liquids* (Oxford University Press, New York, 1987), pp. 263.
16. D.L. Ermak and H. Buckholz, *J. Comput. Phys.* **35** (1980) 169.
17. D.C. Rapaport, *The Art of Molecular Dynamics Simulation* (Cambridge University Press, Cambridge, 1995).
18. H.A. Kramers, *Physica* **7** (1940) 284.
19. W. Schmickler and A. Ignaczak, *Chem. Phys.* **278** (2002) 147.
20. A.M. Kuznetsov, *Charge Transfer in Physics* (Chemistry and Biology, Gordon & Breach, 1995).